## ARTICLES

# Raman-scattering observation of the rutile-to-$CaCl_2$ phase transition in $RuO_2$

S. S. Rosenblum* and W. H. Weber
*Physics Department, MD3028, Ford Research Laboratory, Ford Motor Company, Dearborn, Michigan 48121-2053*

B. L. Chamberland
*Department of Chemistry and Biochemistry, Arizona State University, Tempe, Arizona 85287-1604*
(Received 30 September 1996)

Using a diamond-anvil cell, we have probed the pressure-induced rutile-to-$CaCl_2$ ferroelastic phase transition in $RuO_2$ with Raman spectroscopy. The transition is marked by a splitting of the degenerate $E_g$ mode of the rutile phase into two nondegenerate components and by an abrupt change in the Grüneisen parameters for all the phonons. The behavior of this splitting shows good agreement with Landau's theory for a second-order phase transition, application of which yields a transition pressure of $11.8 \pm 0.3$ GPa. [S0163-1829(97)03326-2]

## I. INTRODUCTION

The low resistivity and reactivity of $RuO_2$ have made it technologically important as a strip-line conductor in integrated circuits, as a diffusion barrier in contact metallizations, and as a catalytic agent.[1,2] Further interest in $RuO_2$ stems from its structural similarity to the geologically important mineral stishovite ($SiO_2$) (see, for example, Haines and Léger[3]): here, the question of whether rutile-structured stishovite transforms into a denser phase has significant consequences in geophysics. As do several other metal dioxides,[4] $RuO_2$ undergoes a pressure-induced rutile ($D_{4h}^{14}, P4_2/mnm$) to $CaCl_2$ ($D_{2h}^{12}, Pnnm$) second-order phase transition.

Under ambient conditions, many $MX_2$ compounds take on either the rutile or the $CaCl_2$ structure.[5] The primary difference between these two structures involves a rotation about the $c$ axis of the $MX_6$ octahedra. From a symmetry point of view, the anions move from sites along the face diagonals in $ab$ planes of the tetragonal rutile structure; to sites off of these diagonals in the lower-symmetry $CaCl_2$ structure. From an atomic packing point of view, the anion layers more closely approach hexagonal close packing in the $CaCl_2$ structure than they do in the rutile structure. Pressure or temperature changes may induce a second-order phase transition between these two phases, with the rutile structure favored at high temperature (larger unit-cell volume) and the $CaCl_2$ structure at high pressure (lower unit-cell volume). In either case, soft-mode behavior is seen near the transition for the vibrational mode whose eigenvector connects the two structures. Nagel and O'Keeffe discussed the soft-mode behavior of the rutile-structured compounds and its relation to the pressure-induced polymorphism.[6] Hyde has argued that the anion-anion, nonbonded interactions determine the relative stability of the two structures,[7] which seems to account for the structural difference between $CaBr_2$ and $CaCl_2$ and a number of rutile-structured fluorides and oxides. However, his model would favor the rutile structure when the nonbonded anion-anion separation distance decreases, which is contrary to what is observed in the pressure experiments.

In this paper, we present a Raman study of the pressure-induced rutile-to-$CaCl_2$ phase transition in $RuO_2$. Neutron and x-ray diffraction are also useful probes of this transition. In diffraction studies, measurements of the unit-cell parameters allow one to calculate the spontaneous strain, $e_{ss}=(a-b)/(a+b)$, which gives a direct window on the order parameter as a function of pressure. In Raman scattering, the onset of this transition can manifest itself not only through the softening of a vibrational mode ($B_{1g}$ in rutile, $A_g$ in $CaCl_2$), but also through the splitting of the degenerate $E_g$ mode of the rutile structure. The splitting of this vibrational mode, which is our primary measure of the transition pressure, relates to the order parameter via the deformation potential.[8] Additionally, we see abrupt changes in the slopes of the frequency-vs-pressure curves for all the phonons at the phase transition.

Several groups[9–12] have used Raman scattering to study temperature-induced phase transitions between the $CaCl_2$ and rutile structures. In $CaBr_2$ and $CaCl_2$, both the expected soft-mode behavior and $E_g$ splitting have been observed in their respective Raman spectra.[9,10,12] $\beta$-$PtO_2$ undergoes the same transition as the former materials,[11] but its ambient pressure $D_{2h}^{12}$ structure is unique among the metal dioxides—most of the latter, particularly the group-VIII metal dioxides, have the $D_{4h}^{14}$ structure. Platinum dioxide can also exist in a rutile phase, $\beta'$-$PtO_2$, which has been synthesized under very high oxygen pressure conditions.[13] This result indicates that oxygen vacancies may serve to stabilize the lower symmetry phase.

In one of the first studies of the pressure-induced $D_{4h}^{14}$-to-$D_{2h}^{12}$ phase transitions, Jorgensen, Worlton, and Jamieson[14] did neutron scattering on $NiF_2$ and found the transition at 1.83 GPa. The first x-ray study of $RuO_2$ (and other rutile materials) under hydrostatic pressure by Hazen and Finger[15] determined the structural changes that take place up to 5.0 GPa. Haines, Léger, and Schulte[4] extended

 

TABLE I. Correlation diagram between the Raman-active modes of the $CaCl_2$ structure and the corresponding modes in the rutile structure.

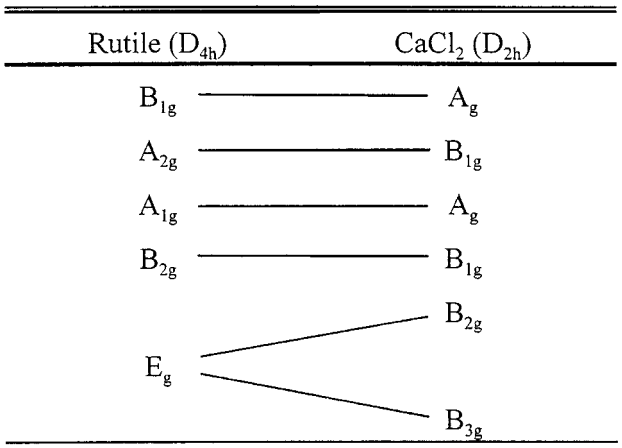


the x-ray work to observe the pressure-induced rutile $\rightarrow CaCl_2 \rightarrow$ modified fluorite $\rightarrow$ orthorhombic $PbO_2$ phase IV $\rightarrow$ cotunnite phase transitions, which occur in a variety of similar materials (only the first three transitions have been observed in $RuO_2$).[3,4,16] In $RuO_2$ they extracted a transition pressure of 5.0 GPa for the second-order, rutile-to-$CaCl_2$ transition, and they observed a first-order, $CaCl_2$-to-fluorite transition beginning at 13.0 GPa.[3]

Merle *et al.*[8] measured the uniaxial-stress dependence of the Raman lines in single-crystal, rutile-phase $TiO_2$ and observed the soft-mode behavior of the $B_{1g}$ phonon and the splitting of the $E_g$ phonon, which occurred when an orthorhombic deformation of the crystal was imposed. In stishovite, Kingma *et al.*[17] used a diamond anvil cell (DAC) to observe both the softening of the $B_{1g}$ mode and the splitting of the $E_g$ mode, which occurred under a hydrostatic pressure of 50 GPa.

## II. EXPECTED MODE BEHAVIOR

In the rutile structure, the metal atoms are located at sites with $D_{2h}$ symmetry ($2a$ in the Wyckoff[18] notation) and the oxygens at sites with $C'_{2v}$ symmetry ($4f$). A factor group analysis[19] yields four Raman active modes: $A_{1g}+B_{1g}+B_{2g}+E_g$; the additional gerade $A_{2g}$ mode is silent. Table I shows the correlation diagram between the modes of the rutile and $CaCl_2$ structures, showing the origin of the latter's six Raman active modes. Traylor *et al.*[20] enumerate the eigenvectors for rutile, and Weber, Graham, and McBride[11] give the eigenvectors for both rutile and $CaCl_2$ as well as a discussion of the changes anticipated as the phase transition is approached.

Rutile transforms to $CaCl_2$ via a *zellengleichen* rotation of the oxygen octahedra about a $c$ axis passing through the metal cations.[21,22] This distortion has the same symmetry as the (rutile) $B_{1g}$ mode, and the latter softens as one approaches the phase transition. Moreover, in rutile materials the $E_g$ splitting, defined as the difference divided by the sum of the two component frequencies, directly relates to the orthorhombic lattice distortion (see Table V of Ref. 8). Thus, we would expect both the soft-mode frequency and the $E_g$ splitting to be proportional to $(P-P_c)^{1/2}$, where $P$ is the hydrostatic pressure exerted on the solid.

## III. EXPERIMENTAL DETAILS

The samples used in this study were among those donated to R. Ward of the University of Connecticut by Engelhard Co. in the 1950s for research on precious metal oxides. The $RuO_2$ crystals, as large as $1\times2$ mm$^2$, were most probably formed using a vapor-phase transport mechanism. These crystals were found to be quite similar to those prepared by Butler and Gillson,[23] who give details of the growth procedure using oxygen as the transporting agent. A subsequent thermal-gravimetric analysis (TGA) on the resulting $RuO_2$ crystals indicated an oxygen to metal ratio of $2.02\pm0.02$.[24] Georg, Triggs, and Lévy[25] also describe the preparation of $RuO_2$ crystals by the oxygen transport method, and their TGA analysis gave an O:Ru ratio of $2.00\pm0.03$. We therefore expect our crystals to be highly stoichiometric.

$RuO_2$ samples smaller than 50 $\mu$m on a side were obtained by fracturing larger crystals. A few of these small fragments, along with some ruby chips, were placed within the 200-$\mu$m hole of a stainless-steel (type 301) gasket mounted to the piston anvil. A Mao-Bell style DAC was used to attain pressures of up to 30.0 GPa.[26] Pressure calibration was done using the ruby fluorescence and was generally accurate to $\pm6\%$.[27] The piston and cylinder were assembled loosely together, and liquid Ar was flowed cryogenically into the gasket and sealed within by applying pressure to the piston. Note that the latter procedure prevented us from choosing the crystal orientation of the sample.

Raman spectra were obtained with a Renishaw Raman microscope, using $\sim6$ mW of HeNe (632.8 nm) radiation. A long working distance $20\times$ objective (Mitutoyo) was used to focus the laser down to about 10 $\mu$m as well as to collect the scattered radiation. This instrument favors the scattered light to have the same polarization as the incident laser beam (i.e., parallel geometry). According to the optical measurements by Goel, Skorinko, and Pollak[28] on $RuO_2$ at ambient pressure, the imaginary part of the refractive index has a value of about unity near 2 eV. The penetration depth for the laser beam is thus about 500 Å, and the sampling depth for the Raman probe is $\sim250$ Å, since the Raman signal must travel back through the sample.

## IV. RESULTS

Figure 1 shows a typical ambient-pressure spectrum obtained in air from a randomly oriented facet on one of the $RuO_2$ crystals. The facet was chosen so that all four modes were observable. The lines observed here are very close to those reported by Huang and Pollak,[29] excepting the $B_{1g}$ mode, which they found as a very weak line at $\sim97$ cm$^{-1}$. We also see this line as being extremely weak, but the frequency is nearly 70 cm$^{-1}$ higher. Unfortunately, the $B_{1g}$ mode, the soft phonon for the phase transition, was too weak to observe inside the DAC. Note that there is a large inelastic continuum under the phonon peaks. Such a background is typical for the electronic Raman scattering from an opaque, conducting material.

We measured the temperature dependencies above room temperature of the lines in Fig. 1, in anticipation of possible

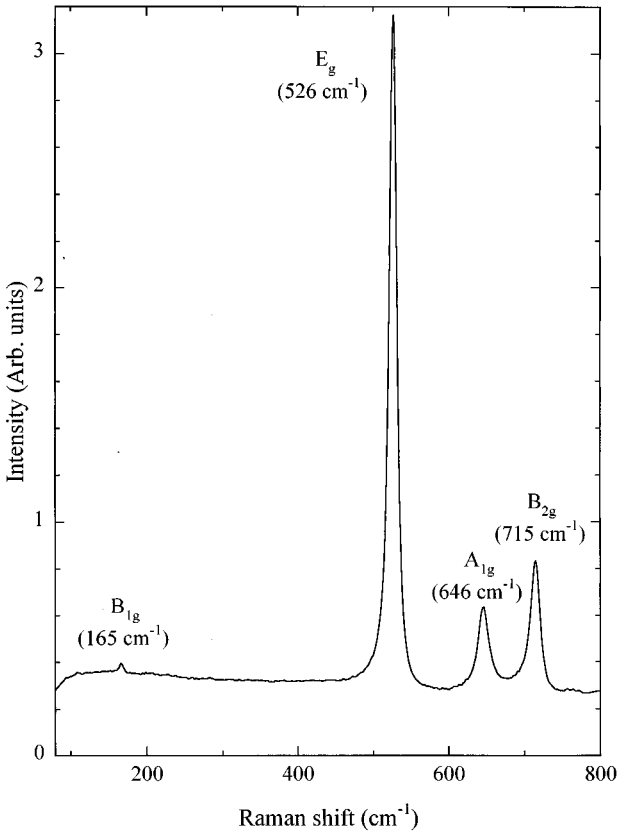


FIG. 1. Ambient pressure Raman spectrum from a single-crystal facet of $RuO_2$ with mode designations for the rutile structure.

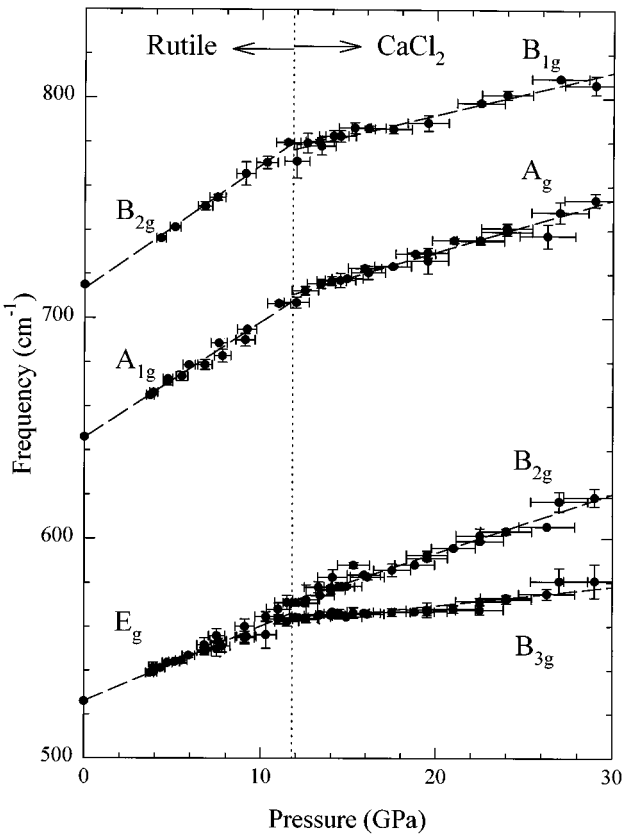


FIG. 2. Plot of phonon frequency vs pressure in $RuO_2$. See text for description of mode assignments. The dotted vertical line at 11.8 GPa denotes the transition from rutile to $CaCl_2$. The dashed lines following the data points are the linear regression lines from which we determined the Grüneisen parameters.

anomalous behavior of the $B_{1g}$ phonon, i.e., an increase in frequency with increasing temperature. No such behavior was seen. All of the modes soften by $\sim 2\%$ as the temperature increased from 16 to 300 °C, indicating that ambient conditions are very far from the phase transition. We have not done polarization measurements on oriented crystals to verify the assignment of the $B_{1g}$ phonon. However, this line was generally weakest when the $E_g$ mode was strongest, and its intensity showed an approximate 90° modulation period when the sample was rotated. Both observations are consistent with $B_{1g}$ symmetry.

At pressures as low as 4.5 GPa, we noticed that some of the $RuO_2$ specimens appeared red under white light. This color change is likely caused by a small, pressure-induced shift in the optical properties, and it need not be related to the structural phase transition. Goel, Skorinko, and Pollak[28] have found that the reflectivity spectrum of $RuO_2$ has a sharp minimum near 2 eV, which means that small changes in the optical constants could easily induce an apparent color change.

The measured pressure shifts of the three strongest lines are shown in Fig. 2. The frequencies are determined by fitting each line to a Lorentzian shape, after subtracting the smooth background. This figure combines results from four loadings of the DAC. Each data point represents an average of two to five spectra obtained at different places on the samples. The vertical error bars are the standard deviations of these averages. The dotted vertical line indicates the transition pressure extracted from our data (see below). The dashed lines are straight line fits to the frequency-vs-pressure data for each line in both phases. Note the marked changes in slopes of these lines that occur at the transition pressure. The mode assignments on the low-pressure side of the figure are for rutile; those on the high-pressure side are for $CaCl_2$.

In Fig. 3 we show the (rutile) $E_g$ mode splitting into ($CaCl_2$) $B_{2g}$ and $B_{3g}$ modes. We have tentatively assigned the lower-frequency peak to the $B_{3g}$ mode, based on the discussion of Weber, Graham, and McBride.[11] They argue, following the results of Merle *et al.*,[8] that the sign of the orthorhombic distortion likely determines the ordering of the $B_{2g}$ and $B_{3g}$ modes. Since the sign of $e_{ss}$ after the phase transition in $RuO_2$ is opposite that in $\beta$-$PtO_2$, we might expect the ordering of the $B_{2g}$ and $B_{3g}$ modes to also be reversed.

The changes with pressure shown in Figs. 2 and 3 are reversible when the pressure is lowered. However, sometimes the linewidths broadened after lowering the pressure, which we attribute to inhomogeneous strain in the pressure medium. We were unable to salvage any of the crystal fragments for further study after a high-pressure run, since the cell depressurized explosively when the gasket seal released.

Finally, in Fig. 4 we plot the square of the splitting vs pressure. As mentioned earlier, the splitting is proportional to the orthorhombic lattice distortion ($e_{ss}$ order parameter). We, therefore, anticipate that the splitting will follow Landau's theory of second-order phase transitions,[30] which means

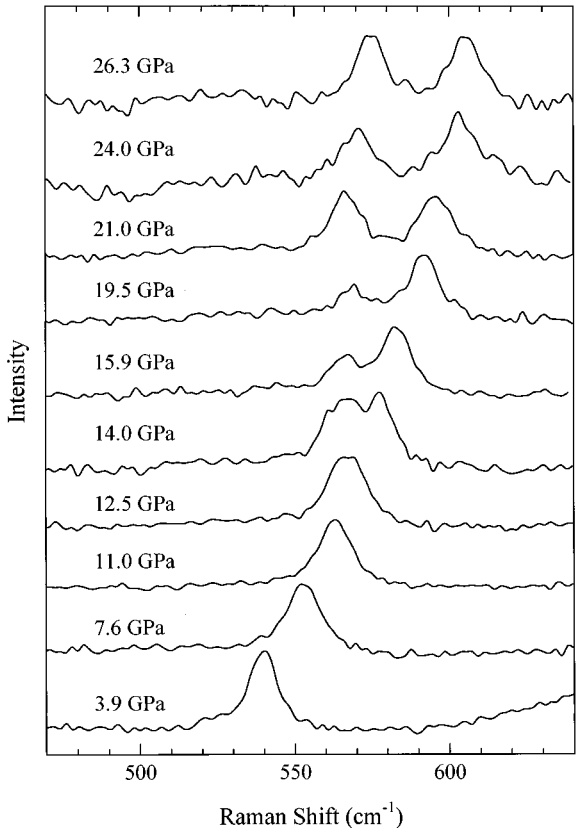


FIG. 3. Raman spectra from $RuO_2$ for a variety of pressures, expanded so as to see only the $E_g \rightarrow B_{2g}+B_{3g}$ splitting. A linear background has been subtracted from each spectrum and the intensity has been scaled for readability.

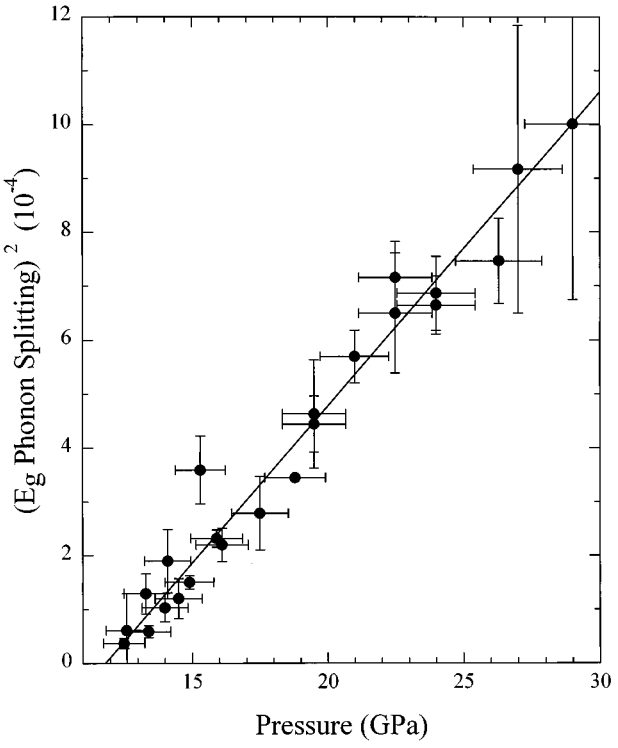


FIG. 4. Plot of the square of the dimensionless $E_g$ splitting (defined as the difference between the two frequencies divided by their sum) vs pressure; the solid line is a linear fit.

it should be proportional to $(P-P_c)^{1/2}$. A least-squares fit of our data to this form, shown by the solid line in Fig. 4, gives $P_c=11.8\pm0.3$ GPa. If we fit the critical exponent $(n)$ along with $P_c$, we obtain $P_c=12.1\pm0.7$ GPa and $n=0.47\pm0.06$.

Table II gives the Grüneisen parameters $\gamma_i$ obtained from the slopes of the phonon-shift versus pressure lines in Fig. 3. These parameters are defined as

$$\gamma_i=(B_0/\nu_i)d\nu_i/dP, \tag{1}$$

where $B_0$ is the isothermal bulk modulus and $P$ is the pressure. For the low-pressure rutile phase we use the value $B_0=270$ GPa, measured by Hazen and Finger.[15] For the high-pressure $CaCl_2$ phase we estimate a value $B_0\sim350$ GPa obtained by fitting a straight line to the cell volume vs pressure data of Hains and Léger[3] for the $CaCl_2$ phase in the range 10–20 GPa. Because of their uncertainty in pressure of $\pm2.5$ GPa, the systematic error in the Grüneisen parameters for the high-pressure phase may be as large as 35%.

## V. DISCUSSION

There are two significant anomalies in our work compared with earlier results. First, we find a much higher frequency for the soft $B_{1g}$ mode—165 $cm^{-1}$ compared to 97 $cm^{-1}$, reported by Huang and Pollak.[29] Second, we find a higher transition pressure for the rutile-to-$CaCl_2$ transition—11.8 GPa compared to 5.0 GPa, reported by Haines and Léger.[3] A possible (and rather speculative) explanation for both effects is that the $RuO_2$ crystals used in the other experiments could be slightly oxygen deficient compared with ours. The work by Herrero-Fernandez and Chamberland[13] on Pt dioxide suggests that oxygen vacancies tend to stabilize the $CaCl_2$ phase. In $\beta'$-$PtO_2$ they found that the reduction of O vacancies actually changed a normally $CaCl_2$-structured compound into one with the rutile structure. If the same mechanism applies to $RuO_2$, then an increased number of oxygen vacancies in the rutile structure will decrease the transition pressure and thus lower the frequency of the soft $B_{1g}$ phonon as measured under ambient pressure. The concept of small changes in O stoichiometry affecting the structure is well known for the layered copper-oxide compounds such as $La_2CuO_{4-y}$ and $YBa_2Cu_3O_{7-y}$,[31,32] but it has yet to be demonstrated for the rutile-structured metal dioxides.

It is also appropriate to compare our Raman results with those from $IrO_2$. Of all the metal dioxides that have the rutile structure and for which Raman data are known, $IrO_2$ is the compound most similar to $RuO_2$. Both materials have a

TABLE II. Grüneisen parameters for the Raman modes of $RuO_2$.

| Rutile structure [a] | | $CaCl_2$ structure [b] | |
|---|---|---|---|
| $A_{1g}$ | 2.19 | $A_g$ | 1.21 |
| $B_{2g}$ | 2.13 | $B_{1g}$ | 0.90 |
| $E_g$ | 1.74 | $B_{2g}$ | 1.74 |
| | | $B_{3g}$ | 0.54 |

[a]Using $B_0=270$ GPa.
[b]Using $B_0=350$ GPa.

nearly half-filled $d$-band electronic structure, and their unit-cell parameters are equal to within 0.04%. The $B_{1g}$ mode in $IrO_2$ was reported by Huang *et al.*[33] to be at 145 $cm^{-1}$, close to our value of 165 $cm^{-1}$. Huang *et al.*[33] also described the $B_{1g}$ mode in $IrO_2$ as being very weak and sharp, which is consistent with our results. We found the full-width at half maximum of the $B_{1g}$ mode at room temperature to be 4.8 $cm^{-1}$, less than half the width of any of the other lines.

Haines and Léger also observed an additional phase transition from the $CaCl_2$ structure to the fluorite ($O_h^5$,$Fm3m$) structure. New x-ray diffraction lines appeared at 11.0 GPa and the unit-cell volume of the new phase, extrapolated to its ambient pressure value, was 8.6% below that for the rutile structure. The Raman spectrum of fluorite would have a single, triply degenerate mode. Although a new mode did not appear above 13.0 GPa in our experiments, this is not proof of the absence of the fluorite phase. Since the $D_{2h}^{12}$-to-$O_h^5$ transition is first order, the two phases will coexist over a range of pressures, and the $D_{2h}^{12}$ Raman lines should be observable over this coexistence region. The fact that the $D_{2h}^{12}$ mode gradually weakened and became unobservable above 30.0 GPa suggests that, indeed, this phase may be disappearing. Alternatively, changes in the material's electronic structure could also explain the decrease in intensity.

In addition to the issue of the O stoichiometry, there are significant differences in the experimental techniques used by us and by Haines and Léger that may contribute to the discrepancies between our results. The x-ray studies used powdered samples, silicone oil for the pressure medium, and Ag diffraction lines for pressure calibration; whereas we used single-crystal samples, argon for the pressure medium, and ruby fluorescence for the pressure calibration. The difference in pressure media is particularly relevant, since Ozaki, Saito, and Kondo[34] have shown that silicone oil becomes highly nonhydrostatic at pressures above 0.8 GPa. An inhomogeneous strain, producing an orthorhombic distortion on some of the grains, would cause the $D_{4h}^{14}$-to-$D_{2h}^{12}$ phase transition to occur at a lower effective hydrostatic pressure.

## ACKNOWLEDGMENTS

We are indebted to G. W. Graham for helping to initiate this work and for participating in its early phases, to B. D. Poindexter for help in adapting the Raman microscope to the diamond anvil cell and for performing the temperature-dependent measurements, and to R. Merlin for the use of the diamond anvil cell. One of us (S.S.R.) thanks Ford Motor Company for financial support.

*Permanent address: Department of Physics, University of Michigan, Ann Arbor, MI 48109-1120.

[1] K. M. Glassford and J. R. Chelikowsky, Phys. Rev. B **49**, 7107 (1994).

[2] O. V. Krasovska, E. E. Krasovskii, and V. N. Antonov, Phys. Rev. B **52**, 11 825 (1995).

[3] J. Haines and J. M. Léger, Phys. Rev. B **48**, 13 344 (1993).

[4] J. Haines, J. M. Léger, and O. Schulte, J. Phys. Condens. Matter **8**, 1631 (1996).

[5] J. K. Burdett, Inorg. Chem. **24**, 2244 (1985).

[6] L. Nagel and M. O'Keeffe, Mater. Res. Bull. **6**, 1317 (1971).

[7] B. G. Hyde, Z. Kristallogr. **179**, 205 (1987).

[8] P. Merle, J. Pascual, J. Camassel, and H. Mathieu, Phys. Rev. B **21**, 1617 (1980).

[9] C. Raptis, R. L. McGreevy, and D. G. Seguier, Phys. Rev. B **39**, 7996 (1989). Note that some mode assignments given here are incorrect; see Refs. 10–12.

[10] Ch. Hahn and H.-G. Unruh, Phys. Rev. B **43**, 12 665 (1991).

[11] W. H. Weber, G. W. Graham, and J. R. McBride, Phys. Rev. B **42**, 10 969 (1990).

[12] H.-G. Unruh, D. Mühlenberg, and Ch. Hahn, Z. Phys. B **86**, 133 (1992).

[13] M. P. Herrero-Fernandez and B. L. Chamberland, J. Less-Common Met. **99**, 99 (1984).

[14] J. D. Jorgensen, T. G. Worlton, and J. C. Jamieson, Phys. Rev. B **17**, 2212 (1978).

[15] R. M. Hazen and L. W. Finger, J. Phys. Chem. Solids **42**, 143 (1980).

[16] J. Haines, J. M. Léger, and S. Hoyau, J. Phys. Chem. Solids **56**, 965 (1995).

[17] K. J. Kingma, R. E. Cohen, R. J. Hemley, and H. K. Mao, Nature (London) **374**, 243 (1995).

[18] R. W. G. Wyckoff, *Crystal Structures*, 2nd ed. (Interscience, New York, 1963), Vol. I.

[19] D. L. Rousseau, R. P. Bauman, and S. P. S. Porto, J. Raman Spectrosc. **10**, 253 (1981).

[20] J. G. Traylor, H. G. Smith, R. M. Nicklow, and M. K. Wilkinson, Phys. Rev. B **3**, 3457 (1971).

[21] L. L. Boyle and J. E. Lawrenson, Acta Crystallogr. Sec. A **28**, 485 (1972).

[22] J. F. Scott, Rev. Mod. Phys. **46**, 83 (1974).

[23] S. R. Butler and J. L. Gillson, Mater. Res. Bull. **6**, 81 (1971).

[24] D. B. Rogers, R. D. Shannon, A. W. Sleight, and J. L. Gillson, Inorg. Chem. **8**, 841 (1969).

[25] C. A. Georg, P. Triggs, and F. Lévy, Mater. Res. Bull. **17**, 105 (1982).

[26] A. P. Jephcoat, H. K. Mao, and P. M. Bell, in *Hydrothermal Experimental Techniques*, edited by G. C. Ulmer and H. L. Barnes (Wiley, New York, 1987).

[27] H. K. Mao, P. M. Bell, J. W. Shaner, and D. J. Steinberg, J. Appl. Phys. **49**, 3276 (1978).

[28] A. K. Goel, G. Skorinko, and F. H. Pollak, Phys. Rev. B **24**, 7342 (1981).

[29] Y. S. Huang and F. H. Pollak, Solid State Commun. **43**, 921 (1982).

[30] L. D. Landau and E. M. Lifshitz, *Statistical Physics*, 3rd ed. (Pergamon Press, New York, 1980).

[31] D. C. Johnston, J. P. Stokes, D. P. Goshorn, and J. T. Lewandowski, Phys. Rev. B **36**, 4007 (1987).

[32] J. D. Jorgensen, M. A. Beno, D. G. Hinks, L. Soderholm, K. J. Volin, R. L. Hitterman, J. D. Grace, I. K. Schuller, C. U. Segre, K. Zhang, and M. S. Kleefisch, Phys. Rev. B **36**, 3608 (1987).

[33] Y. S. Huang, S. S. Lin, C. R. Huang, M. C. Lee, T. E. Dann, and F. Z. Chien, Solid State Commun. **70**, 517 (1989).

[34] Y. Ozaki, S. Saito, and K. Kondo, Jpn. J. Appl. Phys. **10**, 396 (1971).